Final Technical Report

Date of Final Report: December 31, 2006
EPA Grant Number: RD827354C004
Center Name: University of Rochester–EPA PM Center
Center Director: Gunter Oberdorster
Title: Animal Models: Dosimetry, and Pulmonary and Cardiovascular Events
Investigators: Gunter Oberdorster, Alison Elder
Institutions: University of Rochester
EPA Project Officer: Stacey Katz/Gail Robarge
Project Period: June 1, 1999–May 31, 2005 (no-cost extension to May 31, 2006)
Period Covered by the Report: June 1, 1999–May 31, 2006
RFA: Airborne Particulate Matter (PM) Centers (1999)
Research Category: Particulate Matter

Objective(s) of the Research Project: The animal studies (Core 4) were designed to be complementary to the field and controlled clinical studies and to form a link to the mechanistic *in vitro* studies. Furthermore, they were designed to determine pulmonary and systemic responses to inhaled laboratory-generated and real-world ultrafine particles (UFP) and to develop rodent models of human disease to test our central hypothesis that UFP contribute to the increased morbidity and mortality of susceptible individuals in association with small increases in urban particles. Thus, the overall objective of the animal studies was to identify factors that are causally associated with adverse pulmonary and extrapulmonary health effects after low-level exposures to UFP. These factors were hypothesized to include particle size, dosimetry (lung deposition and disposition), host susceptibility (advanced age, cardiovascular disorders, respiratory tract inflammation), and pollutant co-exposure (e.g., ozone).

Two of the main focuses of the Core 4 research were to 1) achieve concordance for the animal studies with the other research cores in terms of endpoints measured and 2) generate and use UFP-containing atmospheres in toxicology studies that are relevant for human ambient air exposures. First, we completed studies in young and old rodents using two different respiratory tract priming agents: inhaled low-dose endotoxin, as a model for pneumonia or exacerbations of COPD, and human influenza virus, a common respiratory pathogen. Intraperitoneally-injected endotoxin was also used in some studies to prime respiratory tract cells from the blood circulation. In addition to creating compromised animal models via specific exposures, we also utilized a genetically-controlled compromised model, namely the SH rat. Several studies were completed in which ozone was used as a co-pollutant, delivered by itself or with laboratory-generated UFP. We also evaluated the clearance kinetics of inhaled UFP in rats with respect to their translocation to extrapulmonary organs across the alveolo-capillary barrier and along sensory neurons from the upper respiratory tract. The particle types used in our studies have included laboratory-generated ultrafine carbon and ultrafine carbon/Fe particles; laboratory-generated organic UFP; concentrated fine/ultrafine particles (ambient Rochester air); and freshly-generated vehicle exhaust emission fine/ultrafine particles on highways. Aside from effects studies in the lungs, we have also focused heavily on cardiovascular and central nervous system

(CNS) responses and on the uptake and tissue-specific distribution of inhaled solid carbon and metal UFP (^{13}C, mixed Mn oxides).

Summary of Findings:

Ultrafine Particle-Containing Atmosphere Generation

Laboratory-Generated Model UFP. As stated above, a main focus of these Core 4 studies was to develop model particles to be used in exposures in animals. We generated ultrafine carbon particles (~26 nm count median diameter [CMD], 15-20 x 10^6 particles/cm^3) and similar UFPs containing ~25% Fe. In addition, ^{13}C UFP were generated for use in particle dosimetry studies. We found that the ultrafine carbon particles have a high surface area (580 m^2/g) as determined via the BET method (Dr. Bice Fubini, Turin, Italy). By aging these particles for 5 minutes, they coagulated into accumulation mode particles with CMD of 280 nm. However, particle surface area remained as high as before. In addition, when rats were exposed to the larger coagulated particles at 2-fold higher concentration than uncoagulated UFP, the inflammatory response was similar to the singlet UFP, possibly due to deagglomeration in the lungs and the available high surface area. Thus, we decided that these coagulated ultrafine particles were not appropriate for use in size comparison studies.

The multigroup studies (described below) were performed with ultrafine carbon particles that were mixed with Fe (25%; i.e., generated from C/Fe graphitized rods). Having completed several of these multigroup studies, we were able to compare responses in animals inhaling ultrafine carbon vs. carbon/Fe particles; we found no evidence to support that *in vivo* inflammatory responses differ when Fe is present in the UFP. This is intriguing given the fact that the Fe in these particles is bioavailable (Dr. Ann Aust, Utah State University) and they generate more hydroxyl radicals in the presence of peroxidethan than do UFP without Fe (Dr. Vincent Castranova, NIOSH). Another interesting point regarding the laboratory-generated UFPs is that they initially contained up to 30% organic material due to a number of plastic components in the spark generator. Efforts to remove all possible sources of contamination in the spark generator were successful so that there was less than 5% of organic carbon in the laboratory-generated UFP aerosol that was used in the studies described below.

Smaller ambient UFP (<~20 nm) consist of organic compounds to a large degree, as seen by our Core 1 measurements. A significant component is used and unused motor oil. Recognizing this, studies were conducted through our Visiting Scientist Program to develop a method for generating organic UFP. To this end, a vaporization-condensation aerosol generator was assembled and characterized by Dr. John Veranth (University of Utah). Used motor oil was used in this system, which was capable of generating stable organic UFP (30-50 nm; 10^6 particles/cm^3) aerosols for 6 hours. Briefly, the motor oil (in hexane and ethyl alcohol) was nebulized such that large droplets were removed by inertial impaction on an impinger, leaving a fine mist that was then directed into a furnace with seed nuclei of NaCl. The oil droplets were completely vaporized and ultrafine aerosols formed when the vapor began to cool at the exit of the furnace. Other studies done with paraffin oil and short-chain alkanes showed that the generation system is adaptable to other low-volatility hydrocarbons.

Generation of Concentrated Ambient Ultrafine/Fine Particles. In addition to these laboratory-generated UFP, we have also performed studies using ambient PM. Through our collaboration with the Harvard PM Center (Dr. Petros Koutrakis), we performed studies using a prototypical UFP concentrator. The prototype sampled air from a moderately busy road adjacent to our laboratory in Rochester and concentrated UFP with some overlap into the fine mode (7-316 nm; CMD=35 nm, GSD=1.9). The average number concentrations during the 6-hour exposures were ~2 x 10^5 particles/cm^3. A state-of-the-art concentrator (Harvard Ultrafine Concentrated Ambient Particle System, HUCAPS) was built and sent to the University of Rochester to be assembled and permanently housed in a new research building for use in controlled animal and clinical exposures to traffic-related aerosols. This system has a 200-nm cutoff, resulting in CMDs of ~75 nm; the gases in the incoming aerosol are neither excluded nor concentrated. Having run the HUCAPS several times, we have found that the number concentration of the output aerosol ranges from 0.05-1.3 x 10^6 particles/cm^3. Figure 1 shows an example of the variation in number concentration and the size distribution in our Rochester facility.

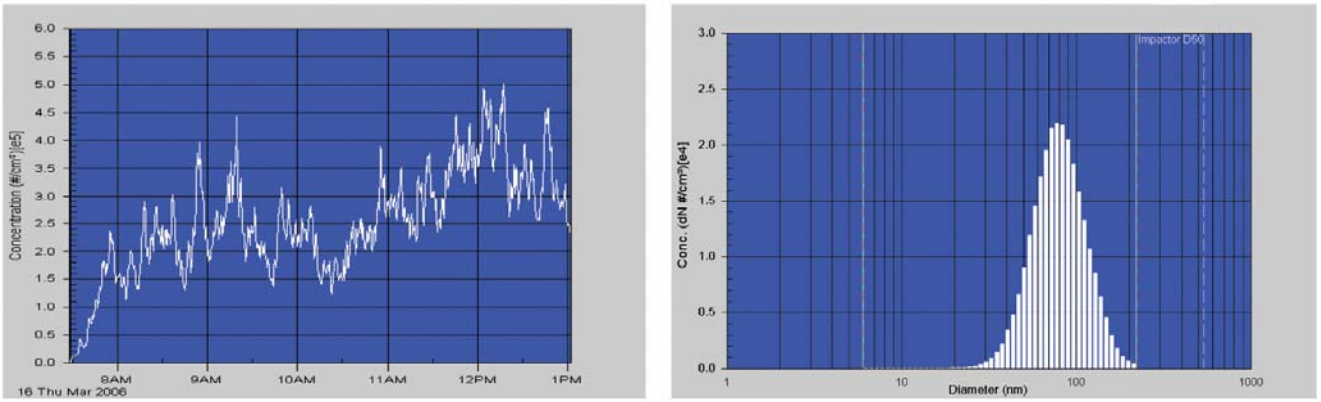

Figure 1. Variation in Particle Number Concentration over a 6-hour Exposure Period (left) and the Particle Size Distribution (right) From the Same Date

Freshly-Generated On-Road Ultrafine/Fine Particles. For toxicological studies with realistic UFP, diluted exhaust from stationary diesel engines or concentrated ambient UFP have been used, yet questions remain about how well these particle dilutions model those found in ambient air. Freshly-generated UFP are present at high concentrations on highways, and vehicle passengers are directly exposed to them when driving behind other vehicles on roads. We exposed rats to such UFP using a mobile emissions laboratory (MEL) from the University of Minnesota (D. Kittelson) for driving rats directly on highways to test the potential of highway aerosols to cause effects when the exhaust from diesel powered trucks was taken in. Since such exposures have not been done before, our objectives were to: (i) demonstrate the feasibility of an on-road exposure study; (ii) determine if there are significant effects in aged rats; and (iii) determine if priming modulates effects in the respiratory tract. A multidisciplinary team approach was used involving PM Center investigators from all of the Research Cores, the Particle Generation and Cardiac Facility Cores, and in collaboration with University of Minnesota scientists (D. Kittelson and W. Watts). Three exposure atmospheres were generated for these studies from the incoming highway aerosol: particles + gas phase, gas phase only, or

particle-filtered and gas-denuded air. The exposures in compartmentalized whole-body chambers consisted of 6 hour driving periods on I-90 between Rochester and Buffalo once or 3 days in a row. The daily average number concentration in the control (filtered air) chamber was 0.01-0.12 x 10^5 particles/cm^3. The in-coming sampled air had a number concentration of 1.95-5.62 x 10^5 particles/cm^3; however, losses were experienced when that air was directed into the chambers, resulting in exposure number concentrations of 0.95-3.13 x 10^5 particles/cm^3. Details about the system itself and the aerosol characterization from our first study using it have been published (Kittelson, et al., 2001, 2004).

One limitation of these studies was the variability in the aerosol number concentration due to both the high dilution factor and long periods of low particle number concentrations. In order to achieve more continuous aerosol sampling, we performed another series of studies with MEL, this time orienting two telescoping pipes on the back of the trailer so that they would sample the engine exhaust plume from the diesel-powered MEL itself as well as—to a lesser degree—those particles and gases from surrounding vehicles. The daily average number concentration in the filtered air chamber was <4.5 x 10^3 particles/cm^3. The in-coming sampled air had a number concentration of 1.6-4.3 x 10^6 particles/cm^3, but some losses were experienced when that air was directed into the chambers. Chamber number concentrations were 4.4-7.6 x 10^5/cm^3, 5.5 to 6.5-fold lower than in-coming air; this same phenomenon was observed in the previous study. The average geometric mean diameter was 15 nm. Despite these losses, the number concentrations in the exposure cages were about twice as high as in the previous study and the in-coming particle number concentration was an order of magnitude higher. The particle number, along with NO and CO_2 concentrations in the incoming air indicated that the MEL exhaust plume was being directly sampled at a dilution of about 400:1.

Toxicology Studies with Laboratory-Generated UFP

Studies in Young and Old Mice Exposed to Combinations of UFP and Ozone with Respiratory Tract Priming. The design for these toxicological studies, unless otherwise specified, involved 16 different groups of animals, representing all possible combinations of exposure components (UFP, ozone, priming agent) and age (young vs. old). Eight groups of young (8-10 weeks) and old (20-22 months) mice and rats were exposed (*n*=5 per group) to UFP (carbon or mixed carbon/Fe) with or without ozone for 6 hours in compartmentalized whole-body chambers with and without prior priming by endotoxin or human influenza virus. Low-dose endotoxin aerosols were used to prime the respiratory tract (~5-10% polymorphonuclear neutrophils [PMNs] in lavage fluid after 24 hours); these priming exposures lasted for~15 minutes and were done immediately prior to UFP/ozone exposures. When human influenza virus (X-31, H3N2; 10^4 EID_{50}) was used as the priming agent, it was intratracheally instilled 48 hours prior to UFP/ozone exposures. We collected all samples for our measurements 24 hours after the start of the UFP/ozone exposure. Since there were four factors involved in these studies, all data were analyzed via four-way analysis of variance (ANOVA) for main effects and interactions between factors. This type of ANOVA is not only the most appropriate one for the study design, but it also has high statistical power.

One "multigroup" study was performed with mixed C/Fe UFP (~100 μg/m^3) and ozone (0.5 ppm) after priming with inhaled low-dose LPS. In agreement with our earlier studies in rats, all

four factors (UFP, ozone, LPS, and age) had significant main effects for most of the respiratory and cardiovascular endpoints examined. The striking age effect was such that inflammatory and cell activation responses in old mice were greater than in young mice. For some endpoints (e.g., lavage PMNs, lavage AM surface ICAM-1 expression), the UFP effect was dependent upon the presence of LPS. This draws attention to the fact that there were several consistent interactions involving inhaled UFP, among them those involving LPS and age (response enhancement) and ozone (response suppression). Our findings that inhaled UFP can alter blood PMN surface ICAM-1 expression are in agreement with results from PM Center-related clinical studies. Some of the most striking effects were observed in lung and heart tissue gene expression changes. Not only were significant alterations in heart tissue gene expression observed, indicating extrapulmonary effects of inhaled UFP and ozone, but the data also suggest an imbalance in old animals between pro-and anti-inflammatory species production (Elder, et al., 2002). Examples for MIP-1α and IL-10 are shown in Figure 2.

Another multigroup study was conducted using influenza virus to prime respiratory tract cells. The design of the study was essentially the same as that of the LPS priming study summarized in the previous section. Young and old male C57 mice (10 weeks, 21 months) were exposed to ultrafine carbon particles containing 25% Fe (CMD ~26 nm, ~140 $\mu g/m^3$) and ozone (0.5 ppm) for 6 hours, alone and in combination. Lung inflammation was induced with intratracheally instilled X-31 human influenza virus 48 hours prior to UFP or ozone exposures. Parameters of inflammation in lavage fluid and blood as well as lavage cell oxidant release were measured 24 hours after exposure. RNA was also extracted from lung and heart tissue for microarray analyses. As before, a 4-way ANOVA was used to analyze the results. UFP were found to have consistent and independent effects on pulmonary inflammation and inflammatory cell activation. Ozone, influenza virus, and age had significant main effects for all endpoints examined. In addition, the interactions with UFP that were consistently significant involved influenza virus, ozone, and age. Using microarray analyses, we have also screened lung and heart tissue for changes in gene expression. There was a trend toward higher pro-inflammatory and lower anti-inflammatory gene expression in tissues from old as compared to young animals. In addition, we found evidence of significant gene changes in heart tissue (Elder, et al., 2004b). When the results from the studies using LPS and influenza virus as priming agents are considered as a whole, a consistent pattern of main effects and factor interactions emerges (see Table 1). Given the fact that there were so many endpoints analyzed in these two sets of studies, the consistency of these interactions is remarkable and strengthens the causality of associations that were found in the statistical analyses. Moreover, the results are also consistent with those of our earlier multigroup studies in young and old rats showing that effects are not species specific.

Table 1. Synopsis of Effects Tests

Multigroup Studies: Synopsis of Effects Tests
(both priming agents/all endpoints)

Main Effects:

UFP	> 1/2 of the endpoints
Ozone	always
Priming Agent	always
Age	all but one endpoint

Consistent Interactions:

UFP interacting with …
- Priming agent
- Ozone
- Priming agent * Ozone
- Priming agent * Age

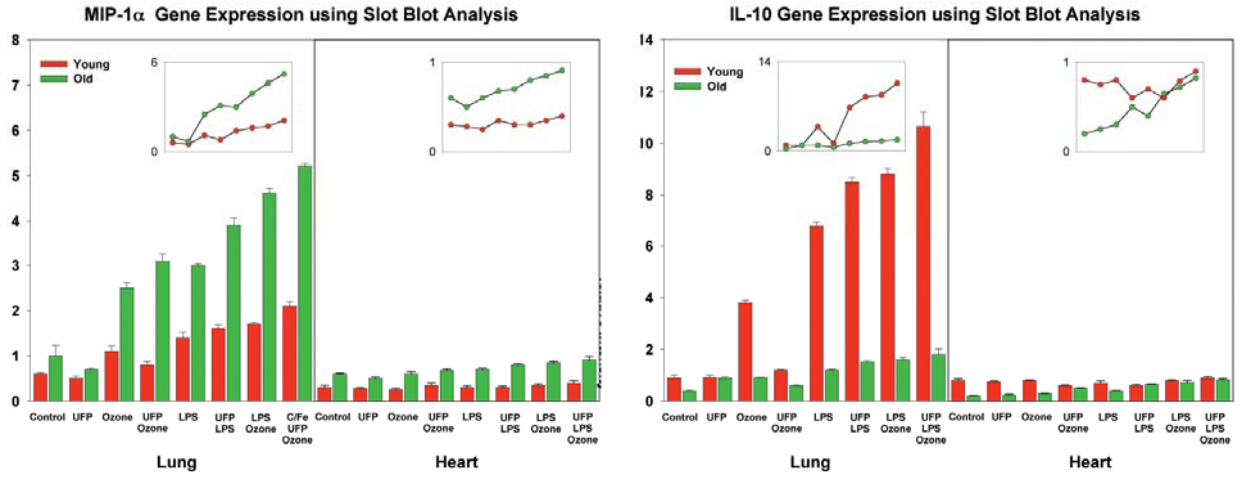

Figure 2. MIP-1α (left) and IL-10 (right) Gene Expression in Lung and Heart Tissue After Exposure to Inhaled UFP in Combination With Ozone After LPS Priming. The insets show line plots of the group means for reference. Responses in young mice are shown in the red bars and those from old mice are shown in green.

Studies with Systemically-Delivered LPS. Other exposures with laboratory-generated ultrafine carbon particles were done after endotoxin priming via ip injection to simulate the early phase of response to an inflammatory stimulus that would prime respiratory tract and circulating cells from the systemic compartment. These studies, however, did not involve ozone. Old F-344 (23 months) and SH (15 months) rats were exposed to UFP for 6 hours, with or without ip LPS priming treatment, which immediately preceded inhalation exposures. Inflammatory lung lavage

and blood parameters were determined, including measurement of intracellular reactive oxygen species (ROS) generation by inflammatory pulmonary and blood cells (oxidation of a fluorescent dye, DCFD). Neither inhaled UFP nor ip LPS caused a significant increase in lavage PMNs or PMA-stimulated ROS release in either animal model, confirming what others have shown about the lung being somewhat protected from systemically-delivered LPS. In F-344 rats, the combination of UFP and ip LPS was suppressive in terms of lavage cell intracellular ROS activity; in SH rats this parameter was not altered by either factor. LPS significantly increased the number of circulating PMNs in both F-344 and SH rats. Interestingly, in F-344 rats, the combination of LPS with UFP led to an enhancement of response, whereas in SH rats, response was suppressed. Blood PMN intracellular DCFD oxidation was affected by exposure in both animal models; however, response was enhanced when UFP and LPS were combined in SH rats and somewhat suppressed in F-344 rats. Plasma fibrinogen was significantly increased by LPS in both animal models. Despite indications that the acute phase response (alterations in plasma fibrinogen) and blood cells were activated, blood viscosity, hematocrit, and coagulability (TAT complex increases) did not change (Elder, et al., 2002, 2004c). The results show that inhaled laboratory-generated UFP did not consistently enhance the LPS response. Although these observations are somewhat limited in scope, they do suggest that 1) the carbonaceous core of ambient PM, as modeled in these experiments, is not solely responsible for cardiovascular effects and 2) the ambient PM-induced alterations in heart rate variability (HRV) found in epidemiological studies can be independent of overt increases in coagulability or acute phase activation.

Effects of Polytetrafluoroethylene (*PTFE) Fumes on Gene Expression in CNS.* We used UFP of known high toxicity to determine changes in CNS gene expression as a basis against which subsequent study results with more benign UFP can be scaled. Our previous work has shown that UFP from inhaled PTFE fumes translocate rapidly to interstitial sites of the lung (Oberdorster, et al., 2000). We conducted exposures with PTFE fumes in order to determine how the translocation of highly toxic UFP affects gene expression in extrapulmonary tissues. The role of biological solubility is not yet known for this particle type. Four SH rats were exposed for 7.5 minutes to PTFE fumes (1.32×10^6 particles/cm^3, 18 nm median diameter, 6.31 μg/L F^-) and four were sham-exposed. This length of exposure resulted in a mild inflammatory response (3.74 ± 1.36 % lavage PMNs) 24 hours after exposure. The lavaged lung as well as heart, liver, olfactory bulbs, cerebrum, and cerebellum were removed for subsequent microarray analysis (J. Carter, Proctor and Gamble Co.). All of the tissues have not yet been analyzed, but results thus far show that ultrafine PTFE fume particles induce significant changes in gene expression in the cerebrum and the olfactory bulb. Genes involved in inflammation (e.g., IL-1, IL-6, TNF-α; 6-to 14-fold changes) are markedly increased relative to sham-exposed rats in both brain regions. Interestingly, a large decrease (25- to 33-fold) in glutamate transporter gene expression was found in both regions after exposure. These changes are remarkable given the fact that they resulted from inhalation of PTFE fumes and that the response in the lung (i.e., %PMNs) was mild. However, we cannot deduce from these results that neuronal translocation of ultrafine PTFE particles *via* the olfactory nerve caused the CNS changes since a systemic inflammatory state might be responsible as well.

<u>Toxicology Studies with Ambient UFP</u>

Studies with Concentrated Ambient Ultrafine/Fine Particles. We conducted several exposures using the prototypical UFP concentrator from the Harvard University PM Center. We performed studies in young and old F-344 rats to measure lung inflammatory processes and lavage cell oxidant release 24 hours post-exposure. The results shown in Figure 3 (analyzed by 2-way ANOVAs per age group) show that the concentrated UFP have significant effects, but that these effects are different in the two age groups. Specifically, the response to the combination of concentrated UFP and LPS in young rats is significantly lower than to LPS alone; the responses in old rats are not significantly different from one another. In old rats, the concentrated UFP alone induced a small, but significant decrease in response as compared to sham-exposed rats; in young rats, the trend is the same, but the two groups are not different from each other. CNS tissues (cerebrum, cerebellum, olfactory bulb, trigeminus) taken from these rats were screened for gene expression changes via microarray analyses. Relative to controls (saline aerosols, sham exposures), no changes were detected in any of the brain regions in those rats (either age group) exposed to concentrated ambient UFP alone. In the olfactory bulb and cerebellum, the expression of several genes (e.g., metallothionein, *i*NOS, IL-6) increased in response to inhaled LPS; these changes were present in both shams and concentrated UFP-exposed groups. Two genes in the trigeminus increased relative to the controls (nerve growth factor, corticotropin-releasing factor). The expression of the two genes increased in olfactory tissue, but not cerebellum, as well. Gene expression appeared to be the same in the two LPS-exposed groups (i.e., no change after concentrated ambient UFP).

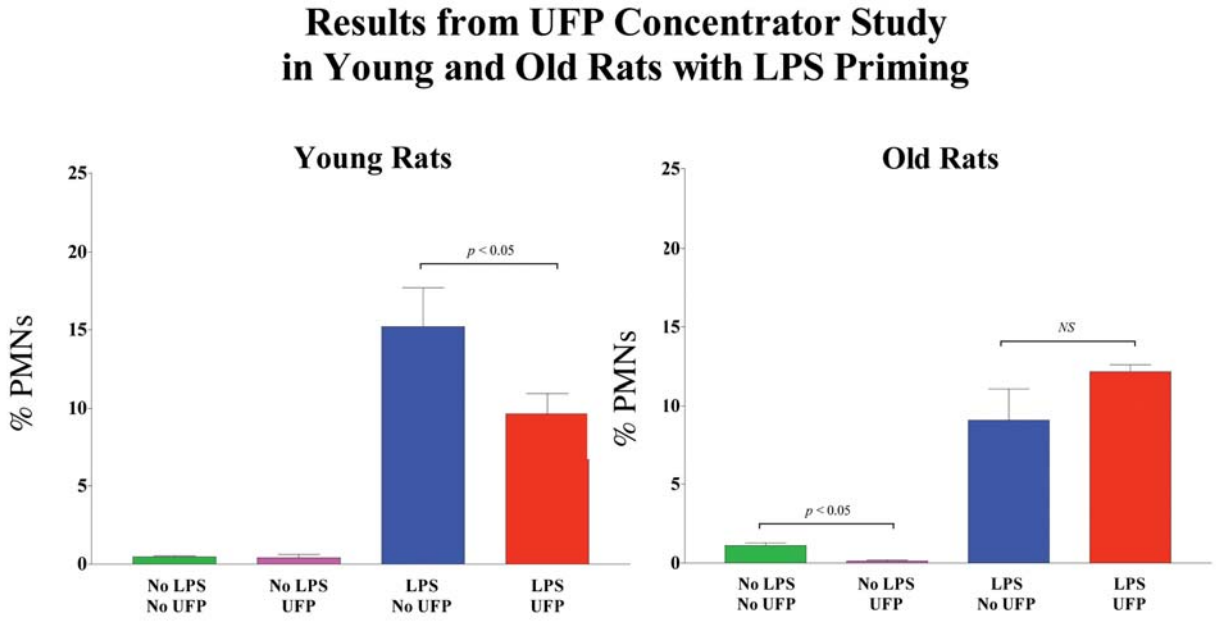

Figure 3. Lavage PMNs 24 Hours After 6-hour Exposures to Concentrated Ambient Ultrafine Particles in Combination With Inhaled LPS Priming in Young (8-10 weeks) and Old (20 months) F-344 Rats

We have now installed the new Harvard Ultrafine Concentrated Ambient Particle System for future studies using compromised animal models and for controlled clinical studies.

Studies with Freshly-Generated On-Road Ultrafine /Fine Particles: Truck Study I. For our studies with real-world UFP from diluted highway exhaust emissions, old rats were pretreated with a low dose of inhaled endotoxin or with instilled influenza virus to induce lung inflammation, as in our studies with laboratory-generated UFP. Endpoints related to lung inflammation, inflammatory cell activation, and acute phase responses were measured after exposure. In addition, two experiments were conducted in telemetered SH rats, one using inhaled and the other injected LPS priming. Heart rate, blood pressure, temperature, activity, and ECG and blood pressure waveforms were continuously recorded for 5 days after exposure (these results are in a subsequent section).

We found that the on-road highway exposures were well-tolerated by rats, as baseline values from sham-exposed animals did not differ from what has been previously published for old F-344 rats; in addition, there were no statistically significant effects of exposure on body weight. Animals were under the constant supervision of personnel in the trailer and no obvious signs of distress were noted during exposure. These results and observations suggest that on-road exposures in mobile laboratories are indeed feasible.

We observed the expected increases in response (inflammation, inflammatory cell activation) to the priming agents. Interestingly, the results suggested no differences in rats exposed to gas-phase components alone vs. the gas-phase + particle mixture. In one study, we found a significant particle-associated increase in plasma endothelin-2 (collaboration with Dr. R. Vincent, Ottawa, Canada), suggesting alterations in vascular endothelial function (Figure 4). In addition, we observed main effects of particles related to the acute-phase response and inflammatory-cell activation. Interactions between on-road particles and the priming agents were also found. The results of these studies appear in Elder, et al., 2004a.

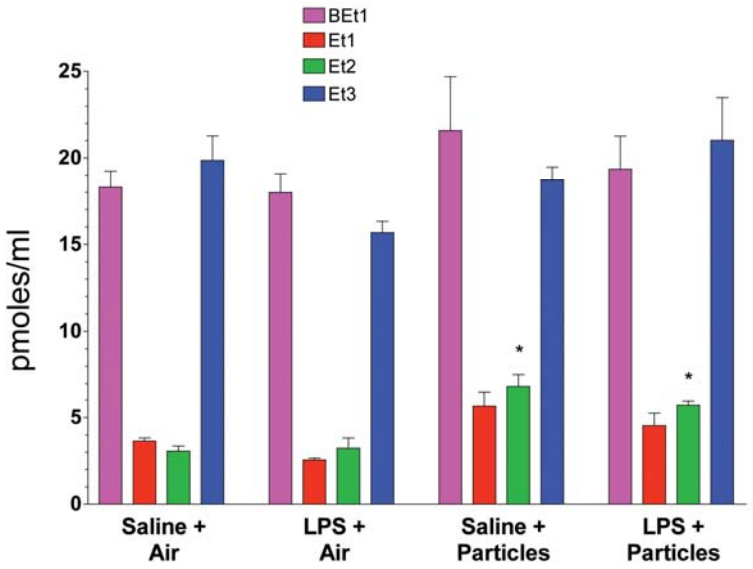

* indicates significant effect of on-road particles, i.e., groups are significantly different from air-exposed counterparts, $p < 0.05$.

Figure 4. Endothelins in Rat Plasma as Determined by HPLC

Studies with Freshly-Generated On-Road Ultrafine /Fine Particles: Truck Study II. Another series of studies was conducted in MEL to obtain more continuous sampling of the emission aerosol. As described above, the truck was configured such that sampling of the truck's own engine exhaust plume could be achieved. As in the previous study, old rats (18-22 month F-344) were exposed directly on highways to either the gas phase/particle mixture, gas phase only, or filtered air. Some were pretreated with a low dose of inhaled endotoxin (immediately prior to on-road exposures) or with instilled human influenza virus (2 days prior to on-road exposures) to induce lung inflammation. Other groups of rats were also exposed to on-road exhaust aerosols first and then to instilled virus. Virus-exposed animals were euthanized 3 days after exposure. The on-road exposures consisted of 6-hour driving periods on I-90 between Rochester and Utica, NY, once or 3 days in a row. Endpoints related to lung inflammation, inflammatory cell activation, and acute phase responses were assessed. In addition, two experiments were conducted in telemetered SH rats. For both experiments, inhaled LPS was used to prime respiratory tract cells. One experiment consisted of a single 6-hour on-road exposure and is similar to the one done in last year's truck study; the second consisted of 3 consecutive days of exposures to the emission aerosols. Telemetry data were collected continuously for 5 days after exposure; data were also collected between each day's exposure for those rats exposed for 3 days in a row (i.e., ~12 hours recorded). The telemetry data are currently being analyzed.

For the parameters that have been analyzed thus far, no differences in response were observed in rats exposed to gas-phase components alone vs. the gas-phase/particle mixture. This was also observed in the previous year's study. We observed the expected responses to the priming agents, e.g., increased percentages of PMNs in bronchoalveolar lavage (BAL) fluid and increased ROS release from BAL inflammatory cells. The exhaust emission aerosols were found to have small but significant effects on several of the endpoints examined thus far. In one experiment, a single 6-hour exposure to on-road aerosols was found to increase the total number of cells in BAL fluid 3 days after exposure in comparison to filtered air controls. In a separate experiment, the aerosols were found to induce a decrease in the percentage of circulating PMNs relative to filtered air controls after a single 6-hour exposure regardless of pre-treatment (LPS or saline aerosol given immediately prior to on-road exposures).

The particle/gas-phase mixture caused an increase in plasma fibrinogen within 24 hours of exposure in influenza-exposed old rats. When the evaluation period was 3 days after aerosol exposure, the mixture caused decreases in fibrinogen. Regardless of priming agent, length of exposure, or length of recovery period, small increases in ICAM-1 surface expression on AMs were found due to the particle/gas-phase mixture. The data also suggest greater message expression for TNF-α and its receptor in lung, heart, and olfactory tissue from those rats exposed to the particle/gas-phase mixture. The effects of the particle/gas-phase mixture were slightly greater and more persistent than those of the gas phase alone. Compared to previous studies in MEL in which the particle number and gas concentrations were lower and less continuous (Elder, et al., 2004a; Kittelson, et al., 2004), we observed here more pronounced effects of freshly-generated vehicle exhaust aerosols, although the specific effects and the directions of the responses were consistent with the earlier study. These results show that freshly-generated

exhaust aerosols have significant effects on the pulmonary and cardiovascular systems in compromised, old rats.

Heart Rate Variability Analyses in Unrestrained, Telemetered SH Rats

Development of a Rat-Specific Algorithm. In parallel to the evaluation of the ECG recordings from the epidemiological and clinical PM Center studies, scientists in our cardiac core have developed an algorithm for analysis of recorded ECG and blood pressure signals from rats. A Windows-based algorithm was developed that was compatible with electrocardiograms and blood pressure signals acquired using the Data Sciences International system (DSI; St. Paul, MN). Based on time and frequency domain approaches, our assessment of HRV relies on a set of parameters known to provide quantitation of autonomic changes. These parameters were standard deviation of NN interval (SDNN), root mean square of successive differences in NN intervals (RMSSD), and the various frequency bands of the power spectrum computed from the tachograms and the systograms (described as low frequency [LF] and high frequency [HF] components). The validation of our algorithm for the quantitation of HRV has been implemented in a similar fashion as previous validation studies, employing pharmacological blockade to dissect the relationship between heart rate (HR), HRV, and blood pressure (BP). Signals are acquired at 1000 HZ sampling frequency with 16 bit amplitude resolution. The preliminary analyses of variability of the HRV parameters led us to conclude that at least 1,500 beats (~5 minutes) are needed to obtain reliable and reproducible estimation of HRV parameters (Couderc, et al., 2002). The first version of our software was based on ECG signals only and results were unexpectedly unstable due to profound and transient changes in QRS wave morphology occurring when the animal was moving in its cage, leading to R-peak misdetection. We thus developed another algorithm for measuring HRV from BP signals, from which we obtained higher stability and reproducibility. Greater morphological stability of the QRS waves was also achieved by placing the negative lead in the musculature surrounding the trachea and the positive lead in the musculature on top of the sternum. With this new lead placement, movement of the rats did not affect the morphology of the QRS complex and our analysis increased in stability.

Test of Analysis Software. The final analysis program has been implemented and tested using positive control data from rats exposed via ip injections to atropine or propranolol, similar to our first study. Two groups of 6 rats were randomized in a cross-over study to receive either of the two agonists or saline. Post-exposure recordings were done for 24 hours. Various time and frequency domain parameters were measured to assess autonomic control when computed from ECG and blood pressure signals. The pharmacological interventions were used to test whether our method identifies sympathetic and parasympathetic blockade. HRV parameters were computed from the tachogram and the systogram and correlations between parameters were computed in order to provide insights into the complex relationship between respiratory activity, heart rate, and blood pressure. Another aim of this study was to better understand the autonomic changes in hypertensive rats. The literature provides controversial results on the autonomic impairment in hypertensive rats. Authors have reported an impaired control of sympathetic drive in comparison to normotensive rats, whereas others revealed reduced vagal tones. Our validation study may help to investigate levels of hypertension and autonomic impairment. Results from this study are presented in a manuscript by Couderc, et al., that is in preparation. The custom

analysis algorithm (Tracking HRV in Electrocardiographic Recordings from Animals using Telemetry, THE RAT) has also been distributed to other investigators (EPA; NYU) in the toxicology field.

Analysis of HRV in Rats Exposed to On-Road Aerosols. The HRV analysis program that was developed and tested by the Cardiology Core was applied to data from telemetered SH rats exposed to on-road aerosols for 6 hours after priming with ip-injected endotoxin or saline. The results suggest that inhaled on-road aerosols activate irritant receptors in the respiratory tract, leading to increased vagal activity. These responses were of greater magnitude and were potentiated in rats pre-treated with endotoxin. Although we did not evaluate arrhythmias, it could be expected that a prolonged and unchecked imbalance favoring parasympathetic drive would lead to bradyarrhythmias. The results showed that heart rate, SDNN, and vagosympathetic balance decreased and the high-and low-frequency components of the power spectrum increased in response to on-road aerosols, suggesting a dysregulation of autonomic input (examples in Figure 5). These findings are the subject of a recently-accepted paper (Elder, et al., 2007). The results suggest that activation of CNS receptors occurs either directly or indirectly by inhaled ultrafine on-road particles and their gaseous co-pollutants. They further suggest, given evidence of parasympathetic activation and the fact that pulmonary irritant receptors are under vagal control, that the observed effects are mediated at the level of the lung as opposed to a systemically-derived response. Further studies with more continuous exposures are needed to confirm these findings.

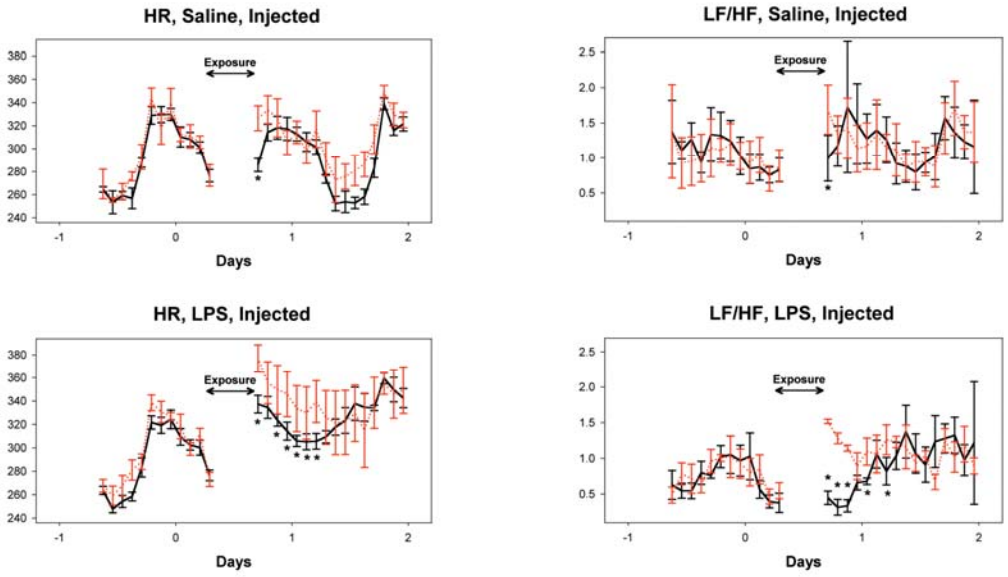

Figure 5. Autonomic Responses (HR, Left; Vagosympathetic Balance, Right) in SH Rats Exposed to Filtered Air (Red) or Freshly-Generated Exhaust Emission Aerosols (Black)

Dosimetry Studies

Translocation of ^{13}C UFP to the Liver. We developed a method to generate ultrafine ^{13}C particles for use in rat dosimetry studies. After several methodological improvements, we performed a study with the objective of determining whether ultrafine elemental carbon particles translocate to the liver and other extrapulmonary organs following inhalation as singlet particles by rats (Oberdorster, et al., 2002). We generated ultrafine ^{13}C particles as an aerosol with CMDs of 20-29 nm (GSD 1.7) using electric spark discharge of ^{13}C graphite electrodes in argon. Nine Fischer-344 rats were exposed to these particles for 6 hours in whole-body inhalation chambers at concentrations of 180 and 80 $\mu g/m^3$; three animals each were killed at 0.5, 18, and 24 hours post-exposure. Six unexposed rats served as controls. Lung lobes, liver, heart, brain (including olfactory bulb), and kidney were excised, homogenized and freeze-dried for analysis of the added ^{13}C by isotope ratio mass spectrometry. Organic ^{13}C was not detected in the ^{13}C particles. The ^{13}C retained in the lung at 0.5 hours post-exposure was about 70% less than predicted by rat deposition models for UFP, and did not change significantly during the 24 hour post-exposure period. Normalized to exposure concentration, the added ^{13}C per gram of lung on average in the post-exposure period was ~9 ng/g organ/$\mu g/m^3$. Significant amounts of ^{13}C had accumulated in the liver by 0.5 hour post-inhalation only at the high exposure concentration, whereas by 18 and 24 hours post-exposure the ^{13}C concentration of the livers of all exposed rats was more than one-third the ^{13}C concentration found in the lung (Figure 6). Although there was a slight increase in ^{13}C in olfactory bulb, no significant increase in ^{13}C was detected in the other organs which were examined. These results demonstrate effective translocation of ultrafine elemental carbon particles to the liver by one day after inhalation exposure. Potential translocation pathways include direct input into the blood compartment from ultrafine carbon particles deposited throughout the respiratory tract as well as uptake into the blood circulation of UFP particles from the GI-tract after swallowing.

Other studies performed within our PM Center's Pilot Programs used ultrafine ^{192}Ir particles. Iridium is the least soluble of metals in the lung and is, therefore, best suited to study its disposition after inhalation. Dr. Kreyling (GSF Munchen) found, in contrast to our results with ultrafine ^{13}C particles, that after intratracheal inhalation exposure, only minimal amounts of ultrafine ^{192}Ir particles were translocated to extrapulmonary organs (Kreyling, et al., 2002). However, it was also found that larger (80 nm) ^{192}Ir particle translocation was 10-fold slower than that of smaller 15 nm ^{192}Ir particles. Collectively, our studies suggest that not only the particle size but also the material and surface properties, like structure and composition, may influence the efficiency of UFP translocation.

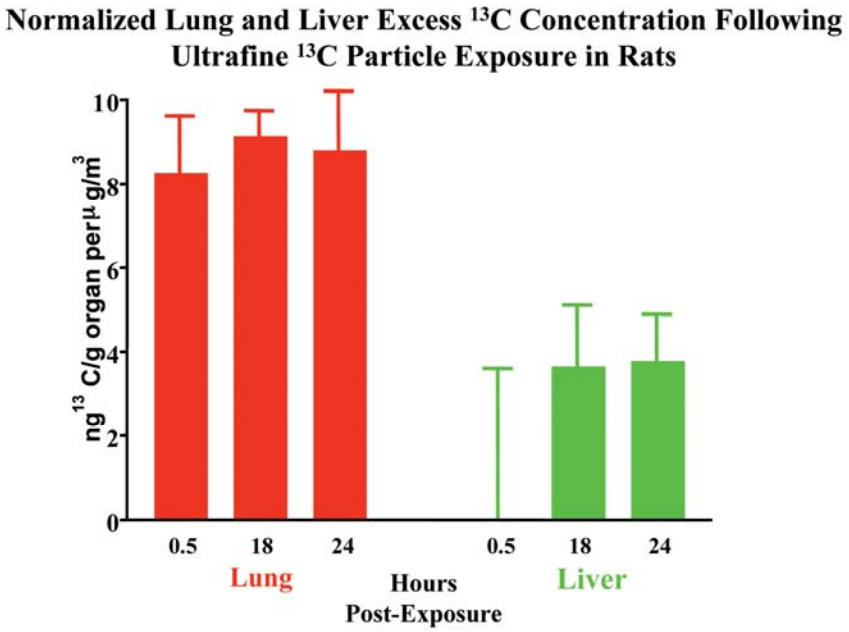

Figure 6. Lung and Liver ^{13}C Concentration in Rats at Different Times After Exposure to Ultrafine ^{13}C Particles, Normalized to the Exposure Concentration

Translocation of ^{13}C UFP to the Brain. A subsequent study with a longer post-exposure period (7 days) showed again significant amounts of added ^{13}C in the liver on day 1, but no longer on day 7. However, on day 7, significant increases in added ^{13}C in heart, brain, and olfactory bulb were found. This prompted us to conduct a follow-up study focusing on uptake of inhaled solid UFP into the CNS, expecting that UFP deposited on the olfactory mucosa of the nasal region will translocate along the olfactory nerve into the olfactory bulb, thereby resulting in high increases in that region as opposed to other areas of the CNS. We generated ultrafine elemental ^{13}C particles (CMD=36 nm; GSD=1.66) from ^{13}C graphite rods by electric spark discharge in an argon atmosphere at a concentration of 160 µg/m^3. Rats were exposed for 6 hours and lungs, cerebrum, cerebellum, and olfactory bulbs were removed after 1, 3, 5, and 7 days. ^{13}C concentrations were determined by isotope ratio mass spectroscopy by Dr. Sharp, our collaborator in these studies at the University of New Mexico, and compared to background ^{13}C levels of sham-exposed controls (day 0). The background corrected pulmonary ^{13}C added as ultrafine ^{13}C particles was 1.39 µg. Lung ^{13}C concentration decreased from 1.39 µg/g (day 1) to 0.59 µg/g (day 7) over the 7-day post-exposure period. There was a significant and persistent increase in added ^{13}C in the olfactory bulb of 0.35 µg/g (day 1) to 0.43 µg/g (day 7) throughout the 7-day post-exposure period with respective ^{13}C levels of 30-40 ng per organ. Day 1 ^{13}C concentrations in cerebrum and cerebellum were also significantly increased but the increase was not always significant over the following days (Figure 7). We conclude from this study that the CNS can be targeted by inhaled UFP and that a neuronal route of translocation of nasally deposited UFP via the olfactory nerve may exist. This represents a previously unrecognized pathway for clearance of solid UFP in the respiratory tract.

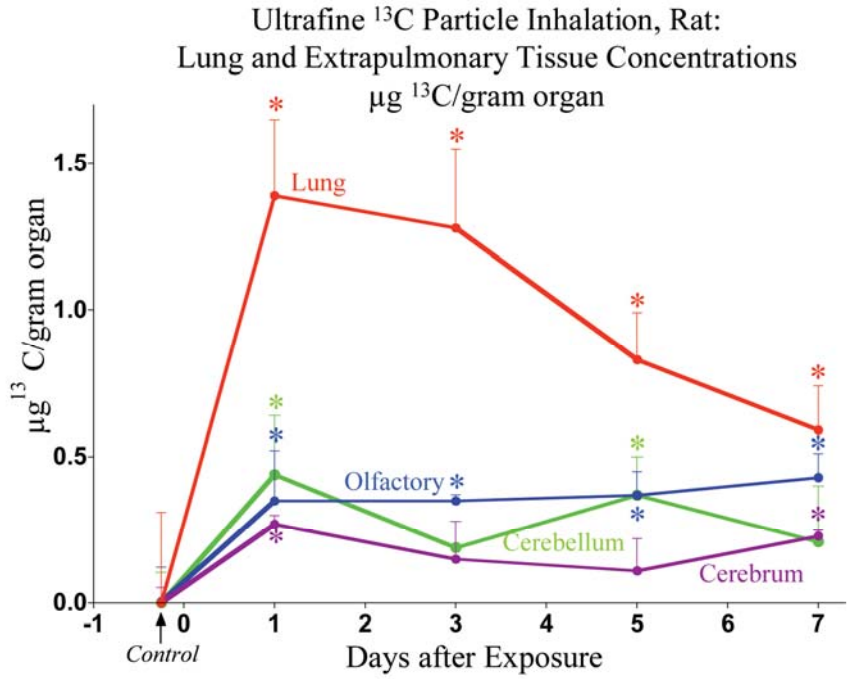

* Significantly increased ^{13}C compared to control levels ($p<0.05$, Dunnet's test).

Figure 7. Translocation of Inhaled Ultrafine ^{13}C Particles to Tissues of the CNS Over 7 Days Post-Exposure

Translocation of Mn Oxide UFP to the Brain. We wished to confirm the olfactory translocation route for inhaled poorly soluble UFP using another material and selected ultrafine Mn oxide because Mn can be sensitively detected by AES, it is a known neurotoxicant, and is of importance for certain occupational exposures where these particles are generated as UFP (metal smelting, welding). Additionally, the EPA has recently confirmed and approved the addition of an organic manganese compound (MMT) to gasoline, thus increasing the potential for human exposures to ultrafine Mn-oxide particles from engine exhaust emissions. We had already developed a system for generating relevant metal UFP, so we made rods for use in the electric spark PALAS generator made from Mn. By introducing a small amount of O_2 into the spark chamber, we were able to generate ultrafine Mn oxide particles (CMD=31 nm; GSD=1.77). Three groups of 3 young F-344 rats were used in these studies. The data from sham-exposed rats were compared to those from rats exposed to the ultrafine Mn oxide particles for 6 or 12 days. Several tissues were harvested after exposure, including the lungs, olfactory bulbs, trigeminal ganglia, striatum, midbrain, frontal cortex, cortex, and cerebellum. Progressive large increases in the Mn content of the olfactory bulb were found (Figure 8), and smaller increases were also seen in striatum and frontal cortex, which are closer to the olfactory bulb. Interestingly, when the right naris was occluded during exposures, Mn accumulated only in the left olfactory bulb, confirming the olfactory nerve translocation pathway. Lung Mn content was slightly more than doubled, but there was no evidence of lung inflammation, as assessed by cellular and biochemical lung lavage parameters. An evaluation of the solubility of the mixed oxides

revealed that <1.5% of the Mn was solubilized per day in physiological saline at neutral pH. A comparison of the translocation to the olfactory bulb of intranasally instilled ultrafine MnO_2 and $MnCl_2$ was also performed and we found that olfactory bulb retention was ~10% of the amount applied regardless of the particle/solute state. In addition, more Mn was retained in the cribriform plate (representative of the olfactory mucosa) when $MnCl_2$ was instilled. These data support the hypothesis that the inhaled Mn oxide UFP are transported in solid particle form by the olfactory nerve. The results from these studies were recently published (Elder, et al., 2006).

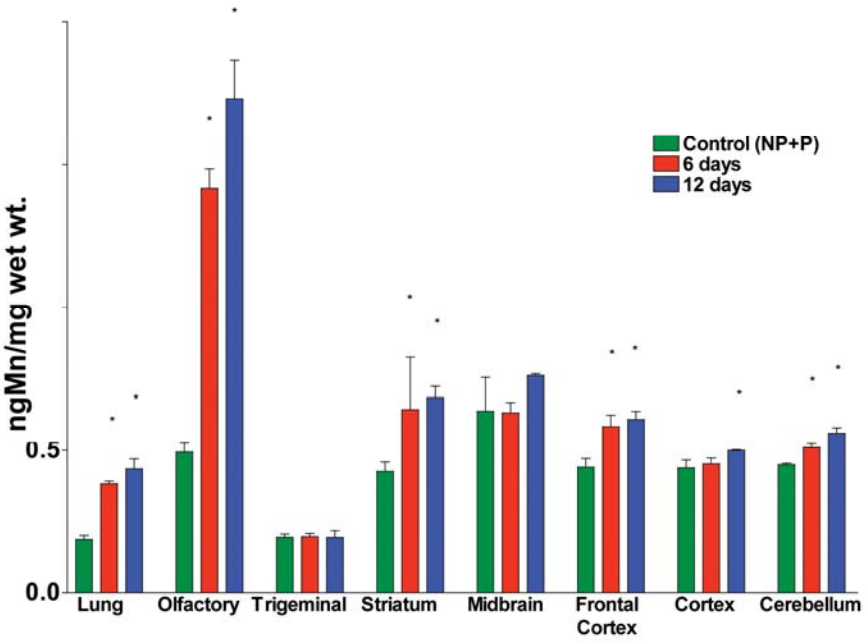

* Indicates significant difference from controls (green bars).

Figure 8. Mn Concentration in Rat Lung and Brain Regions Following 6 and 12 Days of Exposure to Ultrafine MnO_2 Particles (Means ± SD).

Effects of Translocated Mn Oxide UFP. Several tissues (lung, heart, brain regions, etc.) were screened for gene and protein expression changes via microarray and proteomic analyses. Increases in glial fibrillary acidic protein and tumor necrosis factor-α (8-fold increase in message, 30-fold increase in protein), for example, were found in olfactory bulb and, to a lesser extent, in other brain regions where Mn levels were also increased as a result of exposure. These results imply that ambient UFP can potentially affect CNS function, in particular if there is continuous accumulation under even low environmental exposure conditions.

A pilot project was conducted that focused on the potential neurotoxic effects of inhaled UFP in a model of neurodegeneration (MPTP). Mice were exposed to Mn oxide UFP for 3 weeks, after which they were exposed to MPTP to cause injury to dopaminergic neurons in the nigrostriatal regions of the brain. The levels of tyrosine hydroxylase (TH, the rate limiting enzyme for the neurotransmitter dopamine) were measured in striatal tissue following the exposures. Neither

Mn nor MPTP alone significantly lowered striatal TH levels; however, when MN and MPTP were combined, significant reductions were found, suggesting impairment in the production of dopamine in this brain region. Neither exposure component had any effect on parameters of inflammation and cytotoxicity in lung lavage fluid.

Investigations of the Thrombogenic Activity of Inhaled Ultrafine Particles

We optimized a non-invasive method to study the thrombogenic potential of inhaled ultrafine particles. Initial attempts to use the surgically invasive femoral artery or vein model in rats proofed to be of questionable reproducibility, mainly due to manipulation of the blood vessel, causing it to change its tension. We switched to monitoring the ear veins of rats under an inverted microscope. The principle of evaluating a thrombus inducing potential of ultrafine particles involves the local generation of singlet oxygen from i.v. Rose Bengal (RB) by illumination with a green laser beam leading to oxidative endothelial damage. Circulating platelets will adhere, forming a thrombus in the ear vein, which is visible and measurable *in vivo* under the microscope. In the presence of ultrafine particles, the illumination time needed to induce a thrombus is significantly shortened.

Intravenous administration of ultrafine (60 nm) aminated (positively charged)-polystyrene particles (0.02, 0.5, and 50 mg/kg) 30 minutes after the start of the RB infusion significantly shortened the time of thrombus formation in our RB ear model. However, carboxylated (negatively charged) PS particles of the same size failed to affect thrombus formation at any dose. These data suggest that UFP can affect coagulation directly, but that the effect will depend on particle charge (Silva, et al., 2005).

We found that the non-invasive ear vein model also works without the i.v. administration of RB; the green laser alone appears to be sufficient to activate endothelial cells. Intravenous administration of aminated particles in this system showed a significant reduction in the time of thrombus formation. Likewise, intratracheal instillation of the aminated 60 nm PS particles shortened the time to about 42% of the baseline level. These data indicate that ultrafine particles deposited in the respiratory tract can induce changes in thrombus formation without RB and that they might translocate from the lung into the blood stream to produce an effect as shown in our ear vein model.

The thrombogenic potential of more environmentally relevant particles was assessed using the ear vein model. Laboratory-generated ultrafine (30 nm) elemental carbon particles (4, 20, 100, and 500 μg/kg) were administered intravenously to rats and their effects on coagulation studied. It was shown that doses as low as 4 μg/kg (1 μg per rat) were able to significantly (more effective) shorten the time of thrombus formation. The lower doses are significantly different from the high dose, there seems to be a trend indicating that the lower the dose of UFP in the system, the greater the effect. Similar results were obtained when these carbon particles were intratracheally instilled. In this case, even a lower dose (0.8 μg/kg or 0.2 μg per rat) was able to produce a significant effect. These results were presented at the 2005 Society of Toxicology (SOT) meeting by Silva and colleagues. In continuation of these studies, we also observed a thrombogenic effect in rat ear veins following inhalation exposure to either 70 or 200 $\mu g/m^3$ ultrafine carbon for as little as 30 minutes duration.

References:

Couderc J-P, Elder ACP, Cox C, Zareba W, Oberdorster G. Limitation of power spectrum and time-domain analysis of heart rate variability in short-term ECG recorded using telemetry in unrestrained rats. *Computers in Cardiology, IEEE Computer Society Press* 2002;29:589-592.

Elder ACP, Gelein R, Azadniv M, Frampton M, Finkelstein JN, Oberdorster G. Systemic interactions between inhaled ultrafine particles and endotoxin. *The Annals of Occupational Hygiene* 2002;46(Suppl 1):231-234.

Elder ACP, Gelein R, Finkelstein J, Phipps R, Frampton M, Utell M, Kittelson DB, Watts WF, Hopke P, Jeong C-H, Liu W, Zhao W, Zhuo L, Vincent R, Kumarathasan P, Oberdorster G. On-road exposure to highway aerosols. 2. Exposures of aged, compromised rats. *Inhalation Toxicology* 2004a;16(Suppl. 1):41-53.

Elder ACP, Gelein R, Finkelstein J, Frampton M, Utell M, Carter J, Driscoll K, Kittelson, Watts W, Hopke P, Vincent R, Premkumari K, Oberdorster G. Effects of inhaled fine/ultrafine particles combined with other air pollutants. In: Heinrich U, ed. INIS Monographs, 9th Intl. Inhalation Symposium: Effects of Air Contaminants on the Respiratory Tract—Interpretations from Molecules to Meta Analysis, 2004b, pp. 53-68.

Elder ACP, Gelein R, Azadniv M, Frampton M, Finkelstein J, Oberdorster G. Systemic interactions between inhaled ultrafine particles and endotoxin in two rat strains. *Inhalation Toxicology* 2004c;16(6-7):461-471.

Elder A, Gelein R, Silva V, Feikert T, Opanashuk L, Carter J, Potter R, Maynard A, Ito Y, Finkelstein J, Oberdorster G. Translocation of inhaled ultrafine manganese oxide particles to the central nervous system. *Environmental Health Perspectives* 2006;114:1172-1178 (available online: 20 April 2006 (http://dx.doi.org/), doi:10.1289/ehp.9030).

Elder A, Couderc J-P, Gelein R, Eberly S, Cox C, Xia X, Zareba W, Hopke P, Watts W, Kittelson D, Frampton M, Utell M, Oberdorster G. Effects of on-road highway aerosol exposures on autonomic responses in aged, spontaneously hypertensive rats. *Inhalation Toxicology* 2007;19:1-12.

Kittelson DB, Watts WF, Johnson JP. Fine particle (nanoparticle) emissions on Minnesota highways. MN/DOT Report No. 12, 2001. Available at http://www.dot.state.mn.us/research/reports_online.html.

Kittelson DB, Watts WF, Johnson JP, Remerowki ML, Ische EE, Oberdorster G, Gelein RM, Elder AC, Hopke PK, Kim E, Zhao W, Zhou L, Jeong C-H. On-road exposure to highway aerosols. 1. Aerosol and gas measurements. *Inhalation Toxicology* 2004;16(Suppl. 1):31-39.

Kreyling WG, Semmler M, Erbe F, Mayer P, Takenaka S, Schulz H, Oberdorster G, Ziesenis A. Translocation of ultrafine insoluble iridium particles from lung epithelium to extrapulmonary

organs is size dependent but very low. *Journal of Environmental Science and Health. Part A* 2002;65(20):1513-1530.

Oberdorster G, Finkelstein JN, Johnston C, Gelein R, Cox C, Baggs R, Elder ACP. Acute pulmonary effects of ultrafine particles in rats and mice. Health Effects Institute Final Report #96, 2000.

Oberdorster G, Sharp Z, Atudorei V, Elder A, Gelein R, Lunts A, Kreyling W, Cox C. Extrapulmonary translocation of ultrafine carbon particles following inhalation exposure. *Journal of Environmental Science and Health. Part A* 2002;65(20):1531-1543.

Silva V, Corson N, Elder A, Oberdorster G. The rat ear vein model for investigating *in vivo* thrombogenicity of ultrafine particles (UFP). *Toxicological Sciences* 2005;85:983-989.

Supplemental Keywords: NA

Relevant Web Sites: http://www2.envmed.rochester.edu/envmed/PMC/indexPMC.html